Poster 331

Evidence of HIV Evolution in Lymphatic and Cancer Tissues in ART+ Patients

Rebecca Rose[1], Susanna L. Lamers[1], David J. Nolan[1,2], Debra Garcia[3], Marco Salemi[2], Ekaterina Maidj[4], Cheryl Stoddart[4], Elyse Singer[5], Michael S. McGrath[3,4]

[1]Bioinfoexperts, LLC, Thibodaux, LA. [2]University of Florida, Gainesville, FL. [3]The AIDS and Cancer Specimen Resource , [4]University of California at San Francisco, CA; [5]The National Neurological AIDS Bank and the University of California at Los Angeles

Introduction. Anti-retroviral therapy (ART) is effective in reducing plasma HIV load to undetectable levels and restoring partial immunity. However, viral populations rapidly rebound once therapy is removed. Furthermore, risk for certain cancers is increased even with effective ART. We hypothesized that viral populations are maintained in tissues during suppressive ART which may contribute to both rebound virus and on-going pathology.

Table 1. Clinical Details of NNAB/ART+ Patient Cohort. (Further information concerning 20-patient HIV$^+$ART$^+$ cohort is available in poster #345).

NNAB ID	Study number	Years HIV Infected	CSF-VL	Blood-VL	Last Living Blood-VL	Cancer Diagnoses
4149	C01	20	<40	<40	<40	Non-Hodgkin's Lymphoma
5095	C02	3.6	57	<40	<400	Plasmacytoma/Myeloma; Meningio-Encephalitis
4154	C03	13	<40	<40	<40	Anal carcinoma, Non-Hodgkins Lymphoma
4143	C04	4.6	<40	258	<40	Kaposi's Sarcoma, Non-Hodgkins Lymphoma, Kidney Tumor
1010	C05	12.1	338	<40	<400	Basal Cell Carcinoma; Prostate Cancer, Anal Carcinoma, Hepatic Metastasis
NA	KS1	7.7	NA	NA	NA	Kaposi's Sarcoma
NA	KS3	8.5	NA	NA	NA	Kaposi's Sarcoma

Table 2. Highly varied numbers of sequences from assorted tissues were generated for five studied patients The AIDS and Cancer Specimen Resource (ACSR) provided 37 post mortem tissues from five HIV+/ART+ patients with no detectable viral load in CSF and/or cardiac aspirate at autopsy. All patients had brain pathology and cancer. Tissues were assessed for HIV using digital drop PCR and quantitative PCR. Viral RNA and DNA was extracted from HIV+ positive tissue. Sequences were obtained using a single genome amplification approach for the *env* and *nef* genes. *Pol* genes were sequenced in selected additional patients. The number of sequences obtained for each patient/gene is indicated.

Patient	Site	RNA *env*	DNA *env*	RNA *nef*	DNA *nef*	DNA *pol*
C01	Cerebellum	0	0	0	0	NA
	Frontal Cortex	**0**	**0**	**0**	**0**	**NA**
	Basal Ganglia	0	0	0	0	NA
	Meninges	**0**	**0**	**0**	**0**	**NA**
	Occipital	1	0	1	0	NA
	Liver	**0**	**0**	**0**	**0**	**NA**
	Lymph Node (tumor)	0	0	0	0	NA
	Lung	**0**	**3**	**0**	**3**	**NA**
C02	Cerebellum	29	34	30	31	14
	Frontal Cortex	**0**	**17**	**0**	**16**	**16**
	Temporal	0	6	0	6	NA
	Meninges	**0**	**2**	**0**	**2**	**NA**
	Occipital	0	20	0	17	10
	Lymph Node (tumor)	**18**	**22**	**18**	**22**	**14**
	Spleen	0	0	0	0	NA
	Colon	**0**	**0**	**0**	**0**	**NA**
	Kidney	0	0	0	0	NA
	Lung	**0**	**16**	**0**	**19**	**NA**
C03	Kidney	0	0	0	0	NA
	Liver	**0**	**0**	**0**	**0**	**NA**
C04	Cerebellum	0	0	0	0	NA
	Basal Ganglia	**0**	**0**	**0**	**0**	**NA**
	Aorta	0	0	0	0	NA
	Kidney	**0**	**0**	**0**	**2**	**NA**
	Colon	0	9	0	9	1
	Lung	**0**	**26**	**0**	**18**	**8**
C05	Frontal Cortex	0	0	0	0	NA
	Temporal	**0**	**0**	**0**	**1**	**NA**
	Basal Ganglia	0	1	0	1	NA
	Liver (tumor)	**0**	**0**	**0**	**0**	**NA**
	Lymph Node	22	21	15	8	9
	Spleen	**17**	**25**	**15**	**10**	**9**
	Kidney	0	3	0	8	7
	Pancreas	**0**	**2**	**0**	**7**	**NA**
	Aorta	0	0	0	0	NA

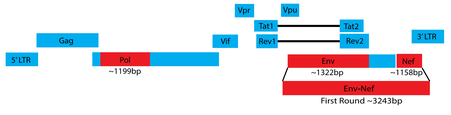
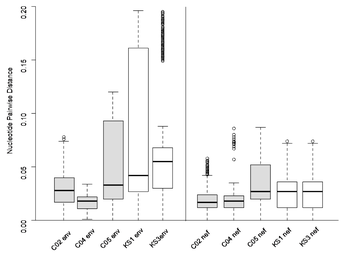


Figure 1. Single genome amplification significantly reduces the chance of duplicate sequences or PCR artifacts. Env-Nef sequences were amplified as a single piece, followed by 2nd round PCR for gp120 env and nef sequences. Tissues positive for env and nef were followed by pol amplification to analyze for drug resistance-associated polymorphisms.

Figure 2. Genetic diversity in ART+ patients was similar to ART- cancer patients. Pairwise nucleotide diversity was measured for the 3 patients with sequences from >2 tissues using the Tamura-Nei model implemented in MEGA. Data from tissue virus sampled from two additional ART- patients (KS1 and KS3) were included for comparison.



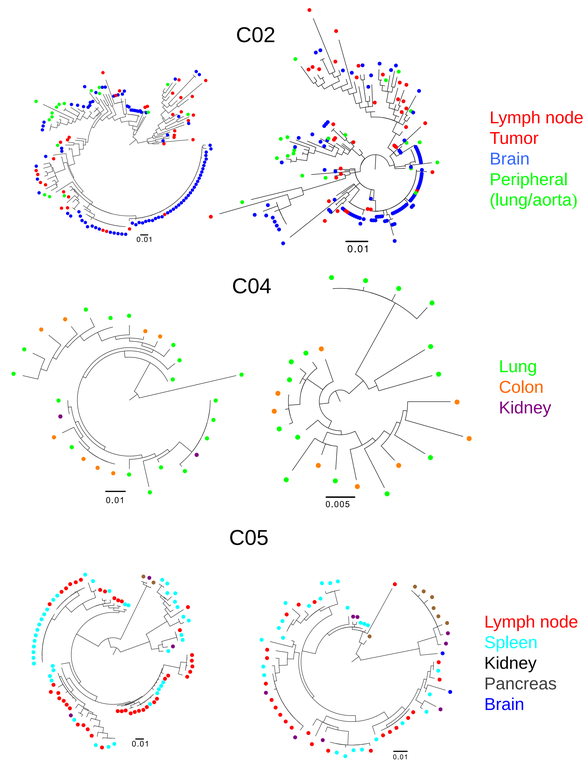


Figure 3. Unrooted phylogenetic trees demonstrate two distinct branching patterns. Maximum likelihood trees were inferred for the *env* sequences (top) and *nef* (bottom) genes for patients C02 (left), C04 (middle) and C05 (right). The GTR+gamma model of nucleotide substitution and NNI+SPR branch swapping methods were implemented in PhyML. Dots at the tips represent sequences colored according to the tissue of origin in the legend. Branches are scaled in substitutions/site according to the bar at the bottom. Clades containing identical sequences and highly evolved sequences were apparent.

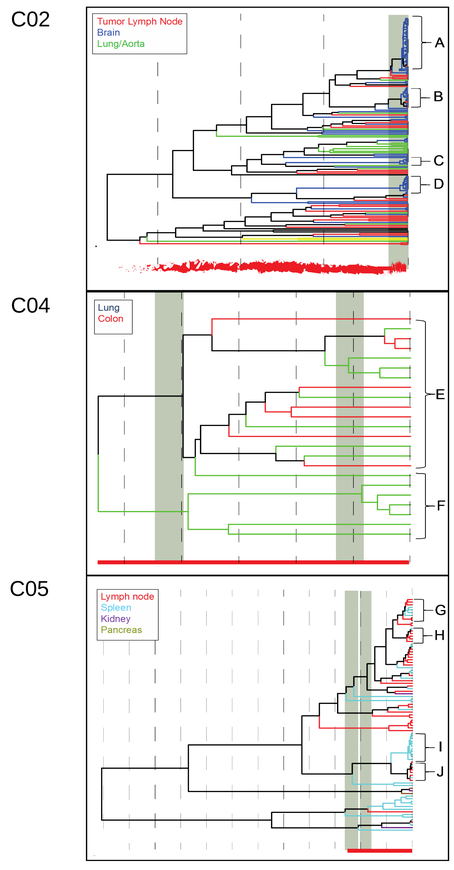
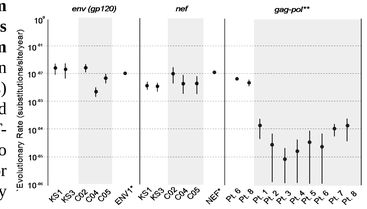


Figure 4. Bayesian time-scaled *env* trees for patients C02, C04, and C05. Branches are scaled in time and colored by tissue from which the sequence was obtained according to the legends. Dotted vertical lines indicate one year. The red line at the bottom of each panel represents the time period during which the patient was on cART. Grey boxes represent cancer diagnoses (six-month window).

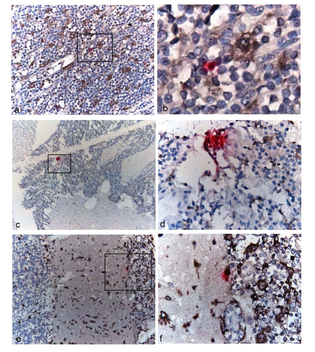
The analysis shows that 1) anatomically dispersed viral populations evolve via different modes of evolution; and 2) periods of increasing lineage diversity correspond to cancer events (grey boxes). In patient C02, many sequences cluster in four distinct clades (A-D), each of which has a very recent common ancestor, whereas the most of the remaining sequences have only a few or no closely related sequences and therefore descend from long terminal branches. For patient C04, the branching pattern is consistent with a constant generation of new lineages. There were two well supported clades, one containing only lung sequences (E), and the other containing lung and colon sequences (F). The patient C05 phylogenies show the pattern of distinct clades with recent common ancestors, which was also evident for patient C02. Most lineage branching events occur within the last two years before death, which correspond to a lymphoma diagnosis. Late in life, this patient's cancer spread to the liver, leading to death, which corresponds in both gene trees with the expansion of clades containing near-identical RNA and DNA sequences from spleen and lymph node (G-J).

Figure 5. Evolutionary rate in tissues from ART+ subjects is not significantly different from tissues from ART- patients; however, it is significantly different from HIV recovered from T-cell populations in ART+ patients. Mean (circle) and 95% confidence interval (vertical bars) evolutionary rates were estimated for the *env* and *nef* regions from the cART-infected and cART-naïve patients in this study (KS1-C05 – KS3). Also shown are the rates reported in Alizon et al* for two regions (ENV1 and NEF) that most closely overlap those studied here; and for the *gag* region as reported in Josefsson**. Black circle = mean rate, vertical bars = 95% confidence interval. Y-axis on log scale. Grey boxes indicate estimates from cART-treated patients.



*Alizon, S. and C. Fraser. Retrovirology, 2013. 10: p. 49.
**Josefsson, L., et al., Proc Natl Acad Sci U S A, 2013. 110(51): p. E4987-96.

Figure 6. RNAscope of cells expressing HIV *gag-pol* transcripts from brain and lymph node tumor of patient C02. Each puncta (pink dot) represents a single HIV *gag-pol* transcript in lymph node tumor (a and b) and cerebellum (c-f). Note that many puncta fuse together and appear as dense red staining of the entire cell. Cells were stained for markers of macrophages (CD68) and activation/infiltration (CD163), brown. Panel b is 630x magnification of the region outlined in panel a. Panels c and f are 400x magnifications of the regions outlined in panels c and e, correspondently. [Panels 4c and d published previously in [26]). HIV RNA is found associated with invasive macrophages in the brain and tumor. Clusters of cells are infected in the brain, potentially corresponding to the large clades of identical brain virus in the phylogenies.



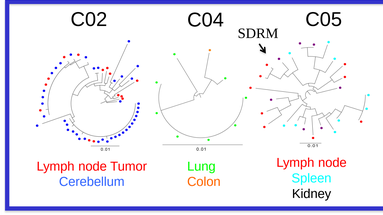


Figure 7. Evolution in tissues could not be explained by drug resistance. Pol sequences show similar evolutionary trends and only one sequence contained a single-nucleotide drug resistance motif.

Conclusions. HIV is present in cancer and pathologic tissues despite low or undetectable viral loads at death. A striking result from this study was the *lack* of a substantial reduction in HIV evolutionary rates in anatomical tissues collected from fully-suppressed cART-treated patients, when compared to viral populations in cART-naïve patients. This pattern differs from that seen in T-cells, in which little or no evolution has been detected. Therefore, an alternative site of viral maintenance during cART, apart from memory T-cells, must be present in order to explain the results presented here. Our data show that lymphatic tissues (e.g. lymph node, spleen), tumor tissue (lymph node) and brain tissue (cerebellum) are sites of replicating virus as evidenced by RNA sequences and mRNA expression of *gag-pol*, and thus may serve as a sanctuary. HIV-infected cells in the brain and lymph nodes are in close proximity to infiltrating activated macrophages, and in some cases the macrophages appear to be infected and expressing HIV. We therefore suggest that macrophages, possibly including tumor-associated macrophages, are the cellular source of the sanctuary and may provide the means of transit for the virus, and protection from the effects of ART.